GIBBS-DONNAN AND SPECIFIC ION INTERACTION THEORY DESCRIPTIONS OF THE EFFECT OF IONIC STRENGTH ON PROTON DISSOCIATION OF ALGINIC ACID.

Carlos Rey-Castro, Roberto Herrero and Manuel E. Sastre de Vicente*.

Departamento de Química Física e Enxeñería Química I, Universidade da Coruña, 15071 A Coruña, Spain.

Corresponding author e-mail: eman@udc.es; fax: +34 981 167065.

Devoted to Prof. Rolando Guidelli on the occasion of his 65th birthday.

Abstract

The apparent proton dissociation constants of a commercial alginic acid have been obtained in KNO_3 and NaCl at concentrations ranging between 0.01 and 2 $mol \cdot L^{-1}$. An analysis of the dependence on the ionic strength at a constant value of the dissociation degree was done by means of empirical functions derived from the Gibbs-Donnan formalism for polyelectrolytes and a specific ion interaction theory (SIT). Both functions were able to fit the experimental data, although SIT yielded rather high errors in the fitted parameters due to a problem of multicollinearity, in contrast to the function derived from the Gibbs-Donnan approach.

Keywords: potentiometry, Gibbs-Donnan model, specific ion interaction theory, alginic acid, equilibrium constants.

1. Introduction

Biosorption, that is, the ability of biomass to sequester heavy metals and other pollutants, has been considered an alternative technique for the removal of toxic metals

from industrial effluents [1]. Among the diversity of materials available, macroalgae have proved to be the most promising biosorbents for heavy metal recovery. The main mechanism of metal sorption to marine algae involves the interaction of the metal cations with the abundant sites of alginate existing in the algae [2, 3]. Therefore, the study of the acid-base chemistry of alginic acid under different ionic strength conditions is a matter of great interest in the field of biosorption, from an environmental point of view.

Alginic acid (AA) is a natural polysaccharide found in brown seaweeds (it may constitute 14 to 40% of the dry solids [4]) that consists of linear chains of 1,4-linked β-D-mannuronic and α-L-guluronic acids [5]. Several studies [6, 7] showed that the acid properties of AA depend on the particular monomer composition.

Specific ion interaction models, such as Guggenheim, Scatchard, or Pitzer models [8], have been successful in describing the ionic strength dependence of the proton binding properties of simple organic ligands like aminoacids [9], amines [10] and carboxylic acids [11-14] in many ionic strength conditions and different background salts.

In the case of natural polyelectrolytes, however, several factors complicate the modeling of the proton binding reactions [15]: a) polyfunctionality (chemical heterogeneity), due to the presence of sites of different nature and/or steric environment; b) possible conformational changes; and c) polyelectrolytic nature, due to the presence of charged functional groups.

A number of papers can be found which deal with the ionic strength dependence of the protonation equilibria of polyelectrolytes. Many of them are focused on the determination of a set of thermodynamic parameters to summarize the experimental data. Simple models have been proposed, such as Katchalsky [16] or Högfeldt [17] models,

which provide successful descriptions of the polyelectrolyte titration curves, although the experimental dependence on the ionic strength of the thermodynamic parameters involved has not a simple theoretical explanation. As a result, different empirical functions have been proposed, often polynomials of the square root of I [18], by analogy with the behaviour of simple ligands. Sammartano and coworkers [19-21] have extensively studied the application of the above-mentioned models to synthetic polyelectrolytes. In a very recent work [22], these authors have also proposed the application of the SIT model to the protonation data of polyacrylic acid.

The available information regarding the proton dissociation of alginic acid is scarce, and only few papers dealing with salt effects can be found [23-25]. The purpose of this work is to analyze the dependence of the AA apparent dissociation constants on the ionic strength by means of two empirical functions derived from the SIT model and the Gibbs-Donnan theory for polyelectrolytes.

2. Models

2.1 Gibbs-Donnan model for a weak acid polyelectrolyte

The similarity between the acid-base behaviour of linear polyelectrolytes and that of their gel analogs has led to the hypothesis that a counterion-concentrating solvent sheath develops around the surface of the charged polyelectrolyte molecule in solution. A two-phase model based on the Gibbs-Donnan formalism has been proposed to explain the properties of these substances by Marinsky and coworkers [26-28].

From the postulates of this model, it has been shown that:

$$\frac{\bar{a}_H}{a_H} = \frac{\bar{a}_M}{a_M} \qquad (1)$$

where a_i is the activity of *i*, M represents the counterion (here, Na^+ or K^+), and the bar indicates an association with the water of the polymer subphase.

The proton dissociation reaction of the polyelectrolyte:

$$AH = A^- + H^+ \qquad (2)$$

can be described by an apparent dissociation constant, $K_{(\alpha)}$, as follows:

$$pK_{(\alpha)} = pa_H - \log\frac{\alpha}{1-\alpha} \qquad (3)$$

where a_H is the proton activity in the bulk solution, and α is the dissociation degree.

The Gibbs-Donnan approach defines an intrinsic equilibrium constant for the dissociation reaction in the polyelectrolyte domain, $\overline{K}$, independent of the bulk ionic strength:

$$p\overline{K}_{(\alpha)} = p\bar{a}_H - \log\frac{\alpha}{1-\alpha} \qquad (4)$$

where now $\bar{a}_H$ corresponds to the proton activity in the polyelectrolyte domain.

The difference between the two constants is given by (pa_M - $p\bar{a}_M$), the so-called Donnan term, which may be regarded as a partition coefficient for the counterion activity between the polymer subphase and the bulk solution:

$$pK_{(\alpha)} = p\overline{K}_{(\alpha)} + \left(pa_M - p\bar{a}_M\right) \qquad (5)$$

If we refer to the corresponding stoichiometric constants, this equation becomes:

$$pK^{*}_{(\alpha)} = p\overline{K}^{*}_{(\alpha)} + \left(pa_M - p\bar{a}_M\right) + \log\left(\frac{\gamma_H}{\bar{\gamma}_H}\right) \qquad (6)$$

where γ_H is the proton activity coefficient.

For the calculation of the Donnan term, the equilibrium of the background electrolyte, MX, between the bulk solution and the hypothetical polymer subphase must be considered:

$$a_M a_X = \bar{a}_M \bar{a}_X \qquad (7)$$

where

$$a_M a_X = \left(m_s + \alpha m_p \phi_p\right)\left(m_s\right)\gamma^2_{\pm MX} \qquad (8)$$

and

$$\bar{a}_M \bar{a}_X = \left(\frac{\alpha V m_p\left(1-\phi_p\right)}{\overline{W}_p} + \overline{m}_s\right)\left(\overline{m}_s\right)\bar{\gamma}_M \bar{\gamma}_X \qquad (9)$$

in these equations m_s represent the molality of the background salt in the bulk solution (equivalent to the molal ionic strength, I, in a 1:1 electrolyte), m_p is the polymer molality, on a monomer basis, ϕ_p is the osmotic coefficient of the salt-free polyelectrolyte, V is the total volume of the solution, $\overline{m}_s$ is the molality of the salt that permeates the polymer domain, and $\overline{W}_p$ represent the amount of water associated with the polymer phase (usually referred to as *Donnan volume*). ϕ_p represents the fraction of counterions that effectively "escapes" from the polyion domain. Under the additivity rule of the colligative properties of simple salt and linear polyelectrolyte solutions, this magnitude is a unique function of α, and almost independent of the ionic strength [29, 30].

In the range of ionic strengths studied, $m_s >> \alpha m_p \phi_p$, due to the high background salt to monomer concentration ratios.

The Donnan term would thus be given by:

$$\frac{\bar{a}_M}{a_M} = \frac{\bar{\gamma}_M}{\gamma_{\pm(MX)}}\left(\frac{\alpha V m_p\left(1-\phi_p\right)}{2\overline{W}_p m_s} + \sqrt{\left(\frac{\alpha V m_p\left(1-\phi_p\right)}{2\overline{W}_p m_s}\right)^2 + \frac{\gamma_{\pm}^{\,2}}{\bar{\gamma}_M \bar{\gamma}_X}}\right) \qquad (10)$$

If the activity coefficient quotients are assumed to be equal to unity, a simplified expression is obtained for the dependence of pK^* on the ionic strength at a constant α:

$$pK^*_{(\alpha)} = p\overline{K}^*_{(\alpha)} + \log\left(\frac{D_{(\alpha)}}{I} + \sqrt{\left(\frac{D_{(\alpha)}}{I}\right)^2 + 1}\right) \qquad (11)$$

where $D_{(\alpha)} = \alpha V m_p(1-\phi_p)/2\,\overline{W}_p$.

In the limit of high ionic strength, where the difference in the counterion concentration between the two phases vanishes, the ratio of the ion activity coefficients is exactly equal to one and, therefore, $\lim_{I\to\infty} pK^*_{(\alpha)} = p\overline{K}^*_{(\alpha)}$. This will be useful for the estimation of $\overline{W}_p$ (see the Results and Discussion section).

$D_{(\alpha)}$ is proportional to the counterion concentration within the polymer phase (not including the permeated salt). This term would be constant for a given α value, provided that $\overline{W}_p$ is constant or a unique function of α. Thus, Eq. (11) constitutes an empirical function that may describe the ionic strength dependence of $pK_{(\alpha)}$ with only two fitting parameters.

Nevertheless, a dependence of $\overline{W}_p$ on both the dissociation degree and ionic strength has been reported for alginic acid [24, 25]. Thus, it would be assumed the next empirical relationship:

$$\frac{\overline{W}_p}{Vm_p} = W'_p = a \cdot \alpha \cdot I^{-b} \qquad (12)$$

where W'_p is used to designate the kilograms of polymer-associated water per mole of monomer.

Substituting Eq.(12) into Eq.(10) gives:

$$pK^*_{(\alpha)} = p\overline{K}^*_{(\alpha)} + \log\left(\frac{D'_{(\alpha)}}{I^c} + \sqrt{\left(\frac{D'_{(\alpha)}}{I^c} \right)^2 + 1} \right) \qquad (13)$$

where c= 1 – b, and $D'_{(\alpha)} = (1-\phi_p)/2a$.

2.2 Application of a specific ion interaction theory (SIT)

The behavior of AA in saline media has been considered according to a single ligand model. For the simple proton dissociation reaction:

$$AH_n^{-z} \Leftrightarrow AH_{n-1}^{-(z+1)} + H^+ \qquad (14)$$

the corresponding thermodynamic equilibrium constant will be given by:

$$K^T = K^* Q(\gamma) \qquad (15)$$

where K^* is the stoichiometric equilibrium constant, K^T its value at infinite salt dilution and $Q(\gamma)$ is the quotient of activity coefficients associated to species appearing in Eq. (14).

According to a Guggenheim-like model for the activity coefficient of the species involved in Eq. (14), the following expression for the dependence of pK^* on the ionic strength, at different degrees of dissociation, is obtained:

$$pK^*_{(\alpha)} = pK^T_{(\alpha)} + \frac{A_{(\alpha)}\sqrt{I}}{1 + B_{(\alpha)}\sqrt{I}} + C_{(\alpha)}I \qquad (16)$$

where pK^T is the value extrapolated to zero ionic strength (note the difference with $p\overline{K}^*$ in the Donnan model), $A_{(\alpha)} = -2 \cdot 0.51 \cdot z_{(\alpha)} \approx -z_{(\alpha)}$ (average charge per molecule of AA), and B, C are parameters related to the mean ionic diameter and the specific binary interactions between species, respectively [8].

It is assumed here that the effective charge (which determines the value of A) and the diameter of the molecule (related to B) are both independent of I, for a given value of α.

Due to the polyelectrolitic nature of AA, it is expected that an analysis of the effect of ionic strength on its acid-base behavior will lead to different values of pK^T at zero ionic strength depending on the dissociation degree. Also, A, B and C in a greater or lesser extent will probably depend on α.

3. Experimental

Alginic acid (free acid from *Macrocystis pyrifera*) was purchased from Sigma-Aldrich, with an approximate composition of 39% of guluronic and 61% of mannuronic acid (data supplied by the manufacturer).

NaCl and KNO_3 (Merck p.a.) were used as background electrolytes to adjust the ionic strength (ranging from 0.01 to 2 $molL^{-1}$) of all the solutions. The HCl, NaOH and

KOH titrating solutions were prepared from the corresponding Merck p.a. reagents and standarized against sodium tetraborate decahydrate (Aldrich) and potassium hydrogen phthalate (Carlo Erba), respectively. The base solutions were prepared in boiled and N_2-purged MilliQ water. The concentrations were accurately calculated from the Gran plots [31], which showed a negligible CO_2 contamination.

Titrations and calibrations were carried out in a glass cell furnished with a thermostating jacket at a temperature of 25.0 ± 0.1 ºC, passing a nitrogen stream through the samples to remove dissolved O_2 and CO_2. The titrating solutions were added from a Crison microBu 2031 automatic buret. Electromotive force measurements were made with a Crison micropH 2000 meter equipped with a Radiometer GK2401C combined glass membrane electrode (Ag/AgCl sat. as reference).

The glass electrodes were calibrated in terms of the proton concentration at a constant ionic strength following the procedure described elsewhere [32, 33]. The calibrations were performed repeatedly for each ionic strength and electrolyte, yielding the formal potential and slope used in subsequent calculations. This method has the advantage that the junction potential and the proton activity coefficient are included in the intercept of the Nernst-type equation [34], so minimizing the possible error due to the change in the medium composition when calibrating the electrode with standard buffers.

For the titrations, 40 or 100 mL of the sample solution (AA at 0.1% or 0.04%, respectively) were placed in the thermostatted vessel and a certain amount of acid was added to yield an initial pH value of ca. 2.5. The automatic buret and pH-meter were computer-controlled by means of a home-made software application. The titration runs were conducted at least in duplicate.

The concentration (in mol·L^{-1}) of the different solutions was converted into molal units through the solution density [35].

The values of the apparent pK at α = 0.3, 0.5 and 0.7 were interpolated from the experimental curves by means of a cubic spline calculated with Origin v.5.0 [36]. The fitting to Eqs. (13) and (16) was performed by the nonlinear least squares minimization tool of Origin v.5.0, based on the Levenberg-Marquardt algorithm.

4. Results and discussion

4.1 pK* vs. α behaviour

Figure 1 shows a sample of the experimental data obtained in NaCl. The pK* vs. α titration curves show a slight shoulder in the central region of α, rather than a smooth and constant increase typical of most polyacids. This behaviour has been reported before for AA and other polyuronic acids by Cesàro and coworkers [7, 37]. These authors discuss the possible simultaneous influence of interchain disaggregation and conformational transitions on the apparent pK behaviour of these substances. Paoletti et al. [38] provided an additional interpretation of such 'bumps' in the $pK_{(\alpha)}$ curves in terms of the counterion condensation theory, for polysaccharides bearing two different carboxylic groups with close pK values.

Regardless of the actual processes occurring throughout the titration, the experimental data can be analyzed by fitting them to empirical models such as the Högfeldt equation, that includes three empirical parameters, pK_0, pK_m and pK_1:

$$pK^*_{(\alpha)} = pK_0(1-\alpha)^2 + 2pK_m(1-\alpha)\alpha + pK_1\alpha^2 \qquad (17)$$

where pK_0, pK_1 are the limit values for $\alpha \rightarrow 0$ and $\alpha \rightarrow 1$, respectively, and pK_m is an intermediate value that accounts for the non-linear behaviour of the function $pK^*_{(\alpha)}$.

The Katchalsky model involves only two parameters, pK_n (equivalent to pK at $\alpha = 0.5$) and n:

$$pK^*_{(\alpha)} = pK_n + (n-1)\log\left(\frac{\alpha}{1-\alpha}\right) \qquad (18)$$

The fitting of the experimental data to Eqs. (17) and (18) is shown in Figure 1 for two particular titrations obtained in NaCl. It can be observed that the three-parameter function describes much better the shape of the titration curve than the two-parameter equation.

From the results obtained, it seems that ionic strength is a more important factor in the apparent equilibrium constant than the dissociation degree (for $0.2 < \alpha < 1$). In fact, the observed values of the slope parameter n in Eq.(18) are relatively small, lying in the range between 1.4 and 1 (the theoretical value for a monomeric acid), and decreasing as ionic strength increases. Polyacrylates, for instance, show values of n between 2.2 and 1.2 in solutions of alkali metal chlorides and nitrates of concentrations between 0.1 and 3 $mol \cdot L^{-1}$ [22].

In theory, the value of the intrinsic equilibrium constant in the Gibbs-Donnan model could be assessed from the extrapolation of the different $pK^*_{(\alpha)}$ curves to $\alpha = 0$. This is the method usually employed in the work of Marinsky and cols. [27]. It is based on the assumption that at $\alpha = 0$ no charge in the macromomolecule is expected, and therefore the

difference between the counterion activities in both phases becomes zero. From Eq. (6) it can be deduced that:

$$pK^{*}_{(\alpha\to 0)} = p\overline{K}^{*}_{(\alpha\to 0)} \qquad (19)$$

The stoichiometric constants must be corrected for the medium effect on the activity coefficients in order to obtain the thermodynamic constants. Once the correction is applied, the curves obtained at different ionic strengths should converge in the limit $\alpha \to 0$.

In practice several factors complicate this procedure. The Donnan model predicts a steep change in $pK^{*}_{(\alpha)}$ at low α values [27]. However, the limitations of the experimental technique (interference of the liquid junction potential on the glass electrode measurements at low pH) hindered the experimental acquisition of data below $\alpha = 0.2$. In addition, the uncertainties in the slope and formal potential of the glass electrode make the error in pK to increase as α decreases. Therefore, the data obtained did not allow to make a reliable extrapolation.

In literature, the extrapolation to $\alpha \to 0$ is often made using a graphical method (see for instance [24]), rather than using a fitting function to estimate the pK value at $\alpha = 0$. The large uncertainties involved in such extrapolation are evident.

Jang et al. [25] did not found a clear convergence of the AA titration curves. Instead, they estimated the intrinsic pK assuming that at a sufficiently high ionic strength all the polyelectrostatic effects are screened. In the case of the present work, this is supported by the fact that the mean slope of the $pK^{*}_{(\alpha)}$ curves decreases as I increases, reaching its lowest value at the highest ionic strength (see the fits to Eq. (18) in Figure 1).

The discussion about the convergence presumes the deviations from the intrinsic constant to be due exclusively to the variable macromolecular charge. However, AA is a natural material with some degree of heterogeneity, and this probably contributes to the shape of the curves. In a greater extent, this effect has been observed in purified peat [39].

4.2 Estimation of the amount of water associated with the polymer phase

In order to derive an analytical expression of $pK^*_{(\alpha)}$ as a function of I, Eq. (13), from the postulates of the Donnan model, it is necessary to introduce an empirical function to describe the variation of W'_p. In this work, a simultaneous influence of α and I, Eq (12), has been considered. This assumption is in contrast, for example, with the typical expression used in the NICA-Donnan model for humic substances [40, 41]:

$$W'_p = a' \cdot I^{-b'} \qquad (20)$$

where a' and b' are two empirical constants independent of pH or α.

The use of Eq. (12) requires further discussion. It has been shown [24, 25] that W'_p can be estimated through use of the Gibbs-Donnan approach. The key point is the assessment of the intrinsic constant. Once $p\overline{K}^*$ is known, the Donnan volume can be obtained by solving Eq. (11) iteratively. In this work, the assessment of $p\overline{K}^*$ by extrapolation to $\alpha \to 0$ was discarded, for the reasons detailed above. Instead, it will be assumed that all the electrostatic effects are suppressed at the highest ionic strength, and thus $pK^*_{(\alpha,\ high\ I)} = p\overline{K}^*_{(\alpha)}$. A similar approach has also been used in the study of proton binding to bacterial cell walls [42] and seaweed biomass [43]. The procedure adopted for

the estimation of the Donnan volume can be summarized as follows: a) the titration curves obtained at different values of I were fitted to Eq. (17); b) the fitted functions were used to interpolate the pK^* data at fixed values of α; c) Eq. (11) was solved iteratively, assuming $pK^*_{(\alpha,\ I=2M)} = p\overline{K}^*_{(\alpha)}$. The values of ϕ_p were taken from bibliography [29], taking into account that the difference between the osmotic coefficients of sodium and potassium alginate can be considered negligible [44]. The results of the calculations for AA in KNO_3 are shown in Figure 2. Some data for AA in NaCl taken from bibliography [24] are included for comparison. The results show an increasing trend with α, especially at low ionic strengths. Both datasets were fitted to Eq. (12), yielding the fitted parameters shown in the legend of Figure 2. The values obtained for b are in agreement with the results listed in Table 2. The fitted functions show a remarkable coincidence between the two electrolytes and provide a satisfactory support for the use of Eq. (12). It is interesting to note that a similar trend in the Donnan volumes has been reported in a study of the proton binding to seaweed biomass [43].

It must be pointed out that when no independent experimental measurements of the specific volume are available, a certain degree of ambiguity in the definition of the electrostatic model may exist [40], and therefore different models for the Donnan volume may lead to equally satisfactory fits of the experimental data [43]. In fact, Eq. (20) would lead to an expression formally identical to Eq. (13), but with a different expression of $D'_{(\alpha)}$. Once again, the empirical nature of Eq. (13), which is proposed only as a useful expression to describe the behaviour of pK^*, must be highlighted.

4.3 Ionic strength dependence

The pK^* values interpolated at α = 0.3, 0.5 and 0.7 are plotted in Figure 3 together with the fits according to Eqs. (13) and (16). The fitted parameters are summarized in Table 1 (SIT) and Table 2 (Donnan).

It can be noted that a good fit was obtained using Eq. (16), in the sense that the function closely follows the trend of the experimental points. Nevertheless, very large errors in parameters A, B and C are obtained, and the pK^T values extrapolated to zero ionic strength show a large uncertainty, probably due to the high sensitivity of the SIT function to errors in the data at low I. The large errors associated to A and B parameters are a result of the presence of multicollinearity among the explanatory variables of the model, which has already been studied in the analysis of the dissociation equilibria of simple ligands [45, 46]. This problem may be expected for this type of ill-defined functions, when the number of experimental points is low, as it has been shown in the above-mentioned works. However, it must be pointed out that the analysis of salt effects using less than ten different ionic strength values is commonplace in most (not only potentiometric) works.

It must also be noted that the highest errors are obtained with AA in KNO_3, where no minimum in $pK^*_{(\alpha)}$ was found within the investigated range of ionic strengths. The presence of a minimum in NaCl, suggested only by the data at the highest ionic strength, entails the use of the linear term in Eq. (16).

The differences in pK^* between both electrolytes, although relatively small, taking into account the reproducibility of the data, follow the trend $K^+ > Na^+$, according to the different complexing ability of the alkali metal cations towards carboxylates [18].

An increase in the parameters A and pK^T on increasing α is observed (Table 1), which might be explained by the growth of the negative charge of AA as the titration

proceeds. Moreover, the increasing trend in B, parameter associated to size, (see Table 1) may be accounted for by the repulsion among negative charges of AA.

In a recent paper regarding the AA dissociation in different sodium salts, Fukushima et al. [23] proposed the application of a Debye-Hückel electrostatic model equivalent to Eq. (16) with C = 0. Their study was restricted to the analysis of pK_n (Eq. (18)) at ionic strengths ≤ 1 M, and no clear evidence of a minimum in $pK^*_{(\alpha)}$ was found. The average charge reported in this work ($z(\alpha=0.5) = 50$ for AA in NaCl) is of a similar order of magnitude than the parameter A listed in Table 1. However, the errors in the parameters are not mentioned by the authors, which makes a precise comparison difficult. They calculated independently a value of 9.6 for the B parameter, from an estimate of the AA molecule radius. This result agrees quite well with the value listed in Table 1.

The Gibbs-Donnan approach has already been applied to the interpretation of the acid dissociation of alginic acid [24, 25], although an explicit function to describe the influence of the ionic strength on the dissociation constant has not been reported. These works agree in their conclusion that alginic acid behaves like a flexible polymer with a sizeable variability in the water content of the counterion-concentrating domain of the polyelectrolyte. The polymer subphase volume estimates reported in these papers for AA in NaCl and $NaNO_3$, respectively, are in agreement with the results of this work, showing an almost linear relationship with α, with an I-dependent slope (see Figure 2). By including this trend (in the form of Eq. (12)) in an equation derived from the Gibbs-Donnan postulates, an empirical expression (Eq. (13)) was obtained which describes satisfactorily the experimental behaviour of $pK^*_{(\alpha)}$ as a function of I (see Figure 3). In addition, this model seems to avoid the presence of multicollinearity and, consequently, the errors in the

optimized parameters are smaller (see Table 2). On the other hand, it does not reflect the presence of a minimum in pK^* insinuated by the results in NaCl shown in this work.

In contrast to the SIT model, the Gibbs-Donnan approach can also be used for the simultaneous description of the dependence of pK^* on I and α, provided that the variation of $p\overline{K}^*_{(\alpha)}$ is properly accounted for [43, 47].

5. Conclusions

SIT and Gibbs-Donnan models have been applied to the study of the ionic strength influence on the proton dissociation of AA in NaCl and KNO_3. Both of them lead to a similar description of the experimental data, although the initial assumptions, the accuracy of the fitted parameters and the thermodynamic information involved are different. The SIT approach essentially represents a methodology analogous to that previously employed in the study of simple ligands, based in the Debye-Hückel theory. This model yields a thermodynamic constant extrapolated to infinite dilution of the background salt and, in the simplest case, two parameters related to the average charge and size of the molecule. The optimized values of the parameters are affected by large errors, due to a problem of multicollinearity.

The Gibbs-Donnan approach, on the contrary, starts from a two-phase model postulated for linear polyelectrolytes and gels, and it leads to a function that includes a dissociation constant extrapolated to high ionic strength and two additional empirical parameters, related to the variation of the water content of the polymer subphase. The values of these parameters, obtained by least squares minimization, show lower associated errors than in the previous case.

6. Acknowledgments

M.S.V. and R.H. would like to express their deep and sincere gratitude to Prof. Guidelli for his scientific guidance and friendship during their stays at Florence.

This work was funded by the projects BQU2002-02133 (from the Ministerio de Ciencia y Tecnología of Spain) and PGDIT02TAM10302PR (from the Xunta de Galicia). C.R.C. benefited from a FPU grant of the Ministerio de Educación, Cultura y Deporte of Spain. The helpful comments from the anonymous reviewers are gratefully acknowledged.

7. References

[1] B. Volesky, Biosorption of heavy metals, CRC Press, Boca Raton, Florida, 1990.

[2] S. Schiewer and B. Volesky, Environ. Sci. Technol., 31 (1997), 1863.

[3] R. H. Crist, J. R. Martin, and D. R. Crist, Environ. Sci. Technol., 33 (1999), 2252.

[4] E. Percival and R. H. McDowell, Chemistry and Enzymology of marine algal polysaccharides, Academic Press, London, 1967.

[5] C. S. Lobban and P. J. Harrison, Seaweed ecology and physiology, Cambridge University Press, Cambridge, 1997.

[6] A. Haug, Acta Chem. Scand., 15 (1961), 950.

[7] A. Cesàro, F. Delben, and S. Paoletti, Int. J. Biol. Macromol., 12 (1990), 170.

[8] M. E. Sastre de Vicente, Curr. Top. Solution Chem., 2 (1997), 157.

[9] S. Fiol, T. Vilariño, R. Herrero, M. E. Sastre de Vicente, and F. Arce, J. Chem. Eng. Data, 43 (1998), 393.

[10] C. Taboada-Pan, I. Brandariz, J. L. Barriada, T. Vilariño, and M. E. Sastre de Vicente, Fluid Phase Equilibr., 180 (2001), 313.

[11] P. G. Daniele, A. De Robertis, C. De Stefano, S. Sammartano, and C. Rigano, J. Chem. Soc. Dalton (1985), 2353.

[12] C. Foti, S. Sammartano, and G. Signorino, Fluid Phase Equilibr., 149 (1998), 91.

[13] J. L. Barriada, I. Brandariz, and M. E. Sastre de Vicente, J. Chem. Eng. Data, 45 (2000), 1173.

[14] C. Rey-Castro, R. Castro-Varela, R. Herrero, and M. E. Sastre de Vicente, Talanta, 60 (2003), 93.

[15] J. Buffle, Complexation reactions in aquatic systems: An analytical approach, Ellis Horwood, Chichester, 1988.

[16] A. Katchalsky, N. Shavit, and H. Eisenberg, J. Polymer Sci., 13 (1954), 69.

[17] E. Högfeldt, J. Phys. Chem., 92 (1988), 6475.

[18] C. De Stefano, S. Sammartano, A. Gianguzza, and D. Piazzese, Talanta, 58 (2002), 405.

[19] C. De Stefano, C. Foti, O. Giuffrè, and S. Sammartano, J. Chem. Eng. Data, 46 (2001), 1417.

[20] C. De Stefano, A. Gianguzza, D. Piazzese, and S. Sammartano, J. Chem. Eng. Data, 45 (2000), 876.

[21] P. G. Daniele, C. De Stefano, M. Ginepro, and S. Sammartano, Fluid Phase Equilibr., 163 (1999), 127.

[22] C. De Stefano, A. Gianguzza, D. Piazzese, and S. Sammartano, React. Funct. Polym., 55 (2003), 9.

[23] M. Fukushima, K. Tatsumi, and S. Wada, Anal. Sci., 15 (1999), 1153.

[24] F. G. Lin and J. A. Marinsky, React. Polym., 19 (1993), 27.

[25] L. K. Jang, N. Harpt, T. Uyen, D. Grasmick, and G. G. Geesey, J. Polymer Sci., 27 (1989), 1301.

[26] J. A. Marinsky, T. Miyajima, E. Högfeldt, and M. Muhammed, React. Polym., 11 (1989), 291.

[27] J. A. Marinsky, in: W. Stumm (Ed.), Aquatic Surface Chemistry. Chemical Processes at the Particle-Water Interface, J. Wiley & Sons, New York, 1987, p. 49.

[28] J. A. Marinsky and M. M. Reddy, J. Phys. Chem., 95 (1991), 10208.

[29] A. Katchalsky, Z. Alexandrowicz, and O. Kedem, in: B. E. Conway and R. Barradas (Eds.), Chemical physics of ionic solutions, J. Wiley, New York, 1966, p. 295.

[30] Z. Alexandrowicz and A. Katchalsky, J. Polymer Sci. A, 1 (1963), 3231.

[31] G. Gran, Anal. Chim. Acta, 206 (1988), 111.

[32] S. Fiol, F. Arce, X. L. Armesto, F. Penedo, and M. E. Sastre de Vicente, Fresenius J. Anal. Chem., 343 (1992), 469.

[33] I. Brandariz, T. Vilariño, P. Alonso, R. Herrero, S. Fiol, and M. E. Sastre de Vicente, Talanta, 46 (1998), 1469.

[34] P. M. May, D. R. Williams, P. W. Linder, and R. G. Torrington, Talanta, 29 (1982), 249.

[35] V. M. M. Lobo and J. L. Quaresma, Handbook of electrolyte solutions, Elsevier, Amsterdam, 1989.

[36] Microcal™ Origin™, v. 5.0, Microcal Software, Inc., Northampton, MA (USA), 1997.

[37] A. Cesàro and M. C. Sagui, Makromol. Chem., Macromol. Symp., 58 (1992), 39.

[38] S. Paoletti, R. Gilli, L. Navarini, and V. Crescenzi, Glycoconjugate J., 14 (1997), 513.

[39] J. A. Marinsky, A. Wolf, and K. Bunzl, Talanta, 27 (1980), 461.

[40] M. F. Benedetti, W. H. van Riemsdijk, and L. K. Koopal, Environ. Sci. Technol., 30 (1996), 1805.

[41] E. Companys, J. Puy, M. Torrent, J. Galceran, and J. Salvador, Electroanalysis, 15 (2003), 452.

[42] A. C. C. Plette, W. H. van Riemsdijk, M. F. Benedetti, and A. van der Wal, J. Colloid Interface Sci., 173 (1995), 354.

[43] C. Rey-Castro, P. Lodeiro, R. Herrero, and M. E. Sastre de Vicente, Environmental Science & Technology (in press) (2003).

[44] A. Katchalsky, R. E. Cooper, J. Upadhyay, and A. Wassermann, J. Chem. Soc., (1961), 5198.

[45] R. Herrero, I. Brandariz, S. Fiol, T. Vilarino, and M. E. Sastre de Vicente, An. Quím, 89 (1993), 602.

[46] S. Fiol, I. Brandariz, R. Herrero, T. Vilariño, and M. E. Sastre de Vicente, Ber. Bunsen. Phys. Chem, 98 (1994), 164.

[47] R. Biesuz, A. A. Zagorodni, and M. Muhammed, J. Phys. Chem. B, 105 (2001), 4721.

Tables

Table 1

Parameters obtained by fitting the experimental $pK^{*}_{(\alpha)}$ data (in the mol·kg^{-1} scale) to Eq.(16). The errors are shown in brackets. [a] σ_{fit}^2 = Σ (Square residuals)/degrees of freedom. [b] the values of C are statistically compatible with zero.

α	$pK^{T}_{(\alpha)}$	A(α)	B(α)	C(α)	$10^3 \cdot \sigma_{fit}^2$ [a]
			AA in KNO_3		
0.3	4.58 (0.25)	-15.7 (6.0)	8.2 (2.2)	-[b]	1.6
0.5	4.54 (0.36)	-14.3 (8.9)	8.5 (3.7)	-[b]	3.1
0.7	5.60 (0.56)	-44 (23)	15.7 (5.1)	-[b]	1.3
			AA in NaCl		
0.3	4.35 (0.14)	-9.4 (2.7)	4.8 (1.3)	0.10 (0.03)	1.0
0.5	4.94 (0.12)	-19.2 (3.2)	8.2 (1.1)	0.09 (0.01)	0.2
0.7	4.90 (0.11)	-16.5 (2.5)	6.84 (0.9)	0.12 (0.02)	0.3

Table 2

Parameters obtained by fitting the experimental $pK^{*}_{(\alpha)}$ data (in the mol·kg^{-1} scale) to Eq.(13). The errors are shown in brackets. [a] σ_{fit}^2 = Σ (Square residuals)/degrees of freedom.

α	$p\overline{K}^{*}_{(\alpha)}$	D'	c	$10^3 \cdot \sigma_{fit}^2$ [a]
		AA in KNO_3		
0.3	2.72 (0.04)	0.37 (0.09)	0.56 (0.04)	1.6
0.5	2.95 (0.02)	0.16 (0.03)	0.70 (0.04)	1
0.7	2.95 (0.02)	0.15 (0.02)	0.75 (0.03)	0.5
		AA in NaCl		
0.3	2.74 (0.04)	0.30 (0.07)	0.61 (0.04)	1.6
0.5	2.88 (0.02)	0.17 (0.03)	0.73 (0.03)	0.8
0.7	2.86 (0.02)	0.18 (0.03)	0.76 (0.04)	1.2

Figure captions

Figure 1

$pK^*_{(\alpha)}$ versus α curves obtained for AA in NaCl. Only four curves are shown, for clarity reasons: 0.01 $mol \cdot L^{-1}$ (squares), 0.05 $mol \cdot L^{-1}$ (circles), 0.20 $mol \cdot L^{-1}$ (diamonds) and 1.0 $mol \cdot L^{-1}$ (up triangles). The lines represent the fits to Eq. (17) (solid line) and Eq. (18) (dashed line), for $\alpha < 0.9$.

Figure 2

Estimates of the amount of water associated to the polymer phase calculated using a Gibbs-Donnan approach. a) Data taken from Lin et al. [24]; b) Data calculated from the results of this work, assuming $pK^*_{(\alpha,\ I=2M)} = p\overline{K}^*_{(\alpha)}$. The lines represent the least-squares fits to Eq. (12).

Figure 3

$pK^*_{(\alpha)}$ values of AA in KNO_3 (a) and NaCl (b) at three different degrees of dissociation: $\alpha = 0.5$ (diamonds), $\alpha = 0.3$ (squares) and $\alpha = 0.7$ (circles). The two latter are shown in the inset for clarity reasons. Data fitted according to Donnan (solid lines) and SIT (dashed lines) models.

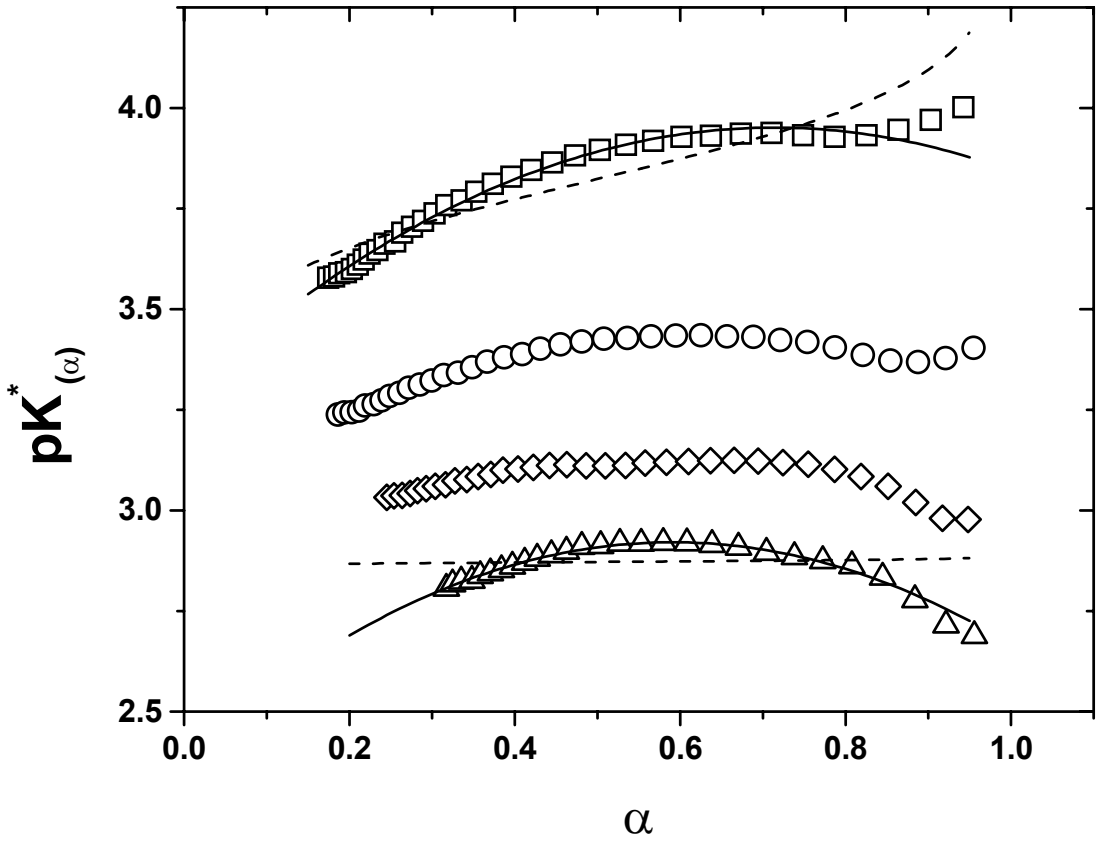

Figure 1

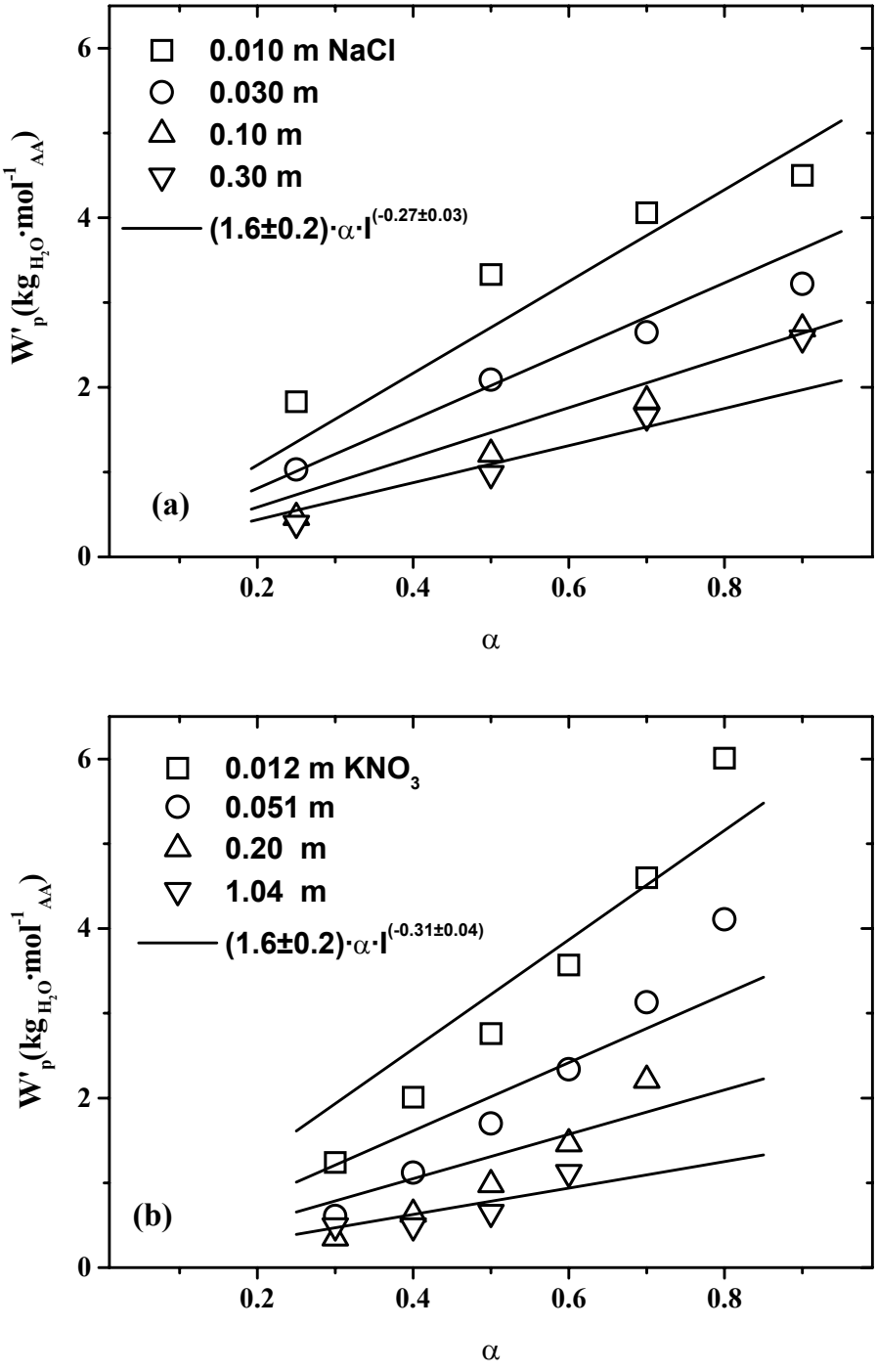
0.010 m NaCl
0.030 m
0.10 m
0.30 m
(1.6±0.2)·α·I^(-0.27±0.03)
(a)
W'p(kgH2O·molAA-1)
α
0.012 m KNO3
0.051 m
0.20 m
1.04 m
(1.6±0.2)·α·I^(-0.31±0.04)
(b)
W'p(kgH2O·molAA-1)
α

Figure 2

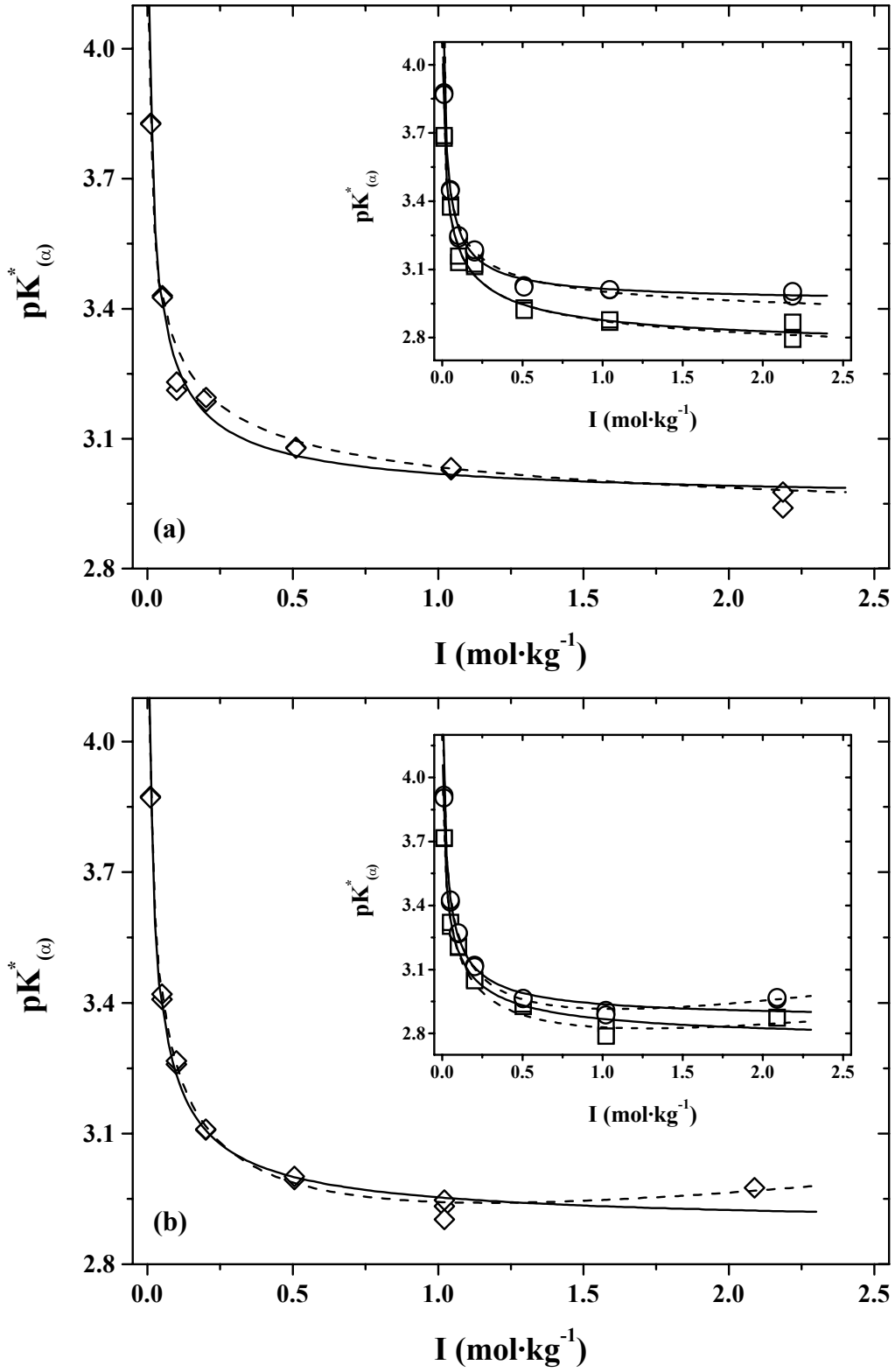

Figure 3